Received: 16 May 2024 | Revised: 15 July 2024 | Accepted: 25 July 2024

DOI: 10.1111/jns.12650

RESEARCH REPORT

WILEY

Automated immunohistochemistry of intra-epidermal nerve fibres in skin biopsies: A proof-of-concept study

Jamie Burgess[1,2] | Anne Marshall[1,2] | Leandros Rapteas[1] | Kevin J. Hamill[1] | Andrew Marshall[1,3] | Rayaz A. Malik[4] | Bernhard Frank[3] | Uazman Alam[1,5,6]

[1]Institute of Life Course and Medical Sciences, University of Liverpool, Liverpool, UK

[2]Liverpool University Hospitals NHS Foundation Trust, Liverpool, UK

[3]The Walton Centre NHS Foundation Trust, Liverpool, UK

[4]Weill Cornell Medicine-Qatar, Doha, Qatar

[5]Department of Cardiovascular and Metabolic Medicine, University of Liverpool, Liverpool, UK

[6]Centre for Biomechanics and Rehabilitation Technologies, Staffordshire University, Stoke-on-Trent, UK

Correspondence
Jamie Burgess and Uazman Alam, Clinical Sciences Centre, Aintree University Hospital, Longmoor Lane, Liverpool L9 7AL, UK.
Email: jamie.burgess@liverpool.ac.uk; uazman.alam@liverpool.ac.uk

Funding information
Versus Arthritis; Pain Relief Foundation

[Correction added on 11 September 2024, after first online publication: The fourth author's name was corrected from 'J. Hamill Kevin' to 'Kevin J. Hamill'.]

Abstract

Aims: To develop a standardised, automated protocol for detecting protein gene product 9.5 (PGP9.5) positive intra-epidermal nerve fibres (IENFs) in skin biopsies, transitioning from the established manual technique to an automated platform. This automated method, although currently intended for research applications, may improve the accessibility of this diagnostic test for small fibre neuropathy in clinical settings.

Methods: Skin biopsies ($n = 274$) from 100 participants (fibromyalgia syndrome $n = 62$; idiopathic small fibre neuropathy: $n = 16$; healthy volunteers: $n = 22$) were processed using an automated immunohistochemistry platform. IENF quantification was performed by blinded examiners, with reliability assessed via a two-way mixed-effects model to evaluate inter- and intra-observer variability.

Results: The automated staining system reproduced intra-epidermal nerve fibre density (IENFD) counts consistent with free-floating sections (mean ± standard deviation: free-floating: 5.6 ± 3.4 fibres/mm; automated: 5.9 ± 3.2 fibres/mm). A median difference of 0.3 with a lower bound 95% Confidence Interval (CI) at −0.00005 established non-inferiority against a margin of −0.4 ($p = .08$). Specifically, the inter-class correlation coefficient (class denotes consistency in measured observations) was 99% (95% CI: 0.9–1), indicating excellent agreement between free-floating and automated methods. The inter- and intra-class coefficient between examiners were both 99% (95% CI: 0.9–0.1) for IENFD, demonstrating high reliability using sections stained using the automated method.

Interpretation: Automated immunohistochemistry provides high-throughput reliable and reproducible intra-epidermal nerve fibre quantification. This method, although currently proof-of-concept, for research use only, may be more widely deployed in histopathology laboratories to increase the adoption of IENFD assessment for the diagnosis of peripheral neuropathies.

KEYWORDS
automated, density, digital pathology, fibromyalgia syndrome, immunohistochemistry, intra-epidermal nerve fibres, pathology, quantification, small fibre neuropathy

1 | INTRODUCTION

A recent scoping review identified 73 human diseases in which intra-epidermal nerve fibre density (IENFD) was affected in studies quantifying cutaneous nerves in a standardised manner using protein gene product 9.5 (PGP9.5).[1] Indeed, intra-epidermal nerve fibre quantification in skin biopsies is considered a reliable diagnostic tool for identifying small-fibre neuropathies.[2] Skin biopsies are routine procedures frequently used for the diagnosis of skin conditions.[3] The development of a method to quantify IENFD[4] and the creation of a normative reference range[5] have positioned skin biopsy and IENFD assessment as the de facto diagnostic reference standard for small fibre neuropathy (SFN).[6,7]

Currently, free-floating sections are prepared according to published recommendations to identify PGP9.5 positive cutaneous nerve fibres[8] and autonomic innervated structures[8] in skin biopsy specimens. Indeed, seminal contributions by Lauria and colleagues have established a robust foundation.[5,8–15] Manual free-floating section methods yield excellent staining outcomes which, with expertise, have minimal handling and staining artefacts. However, such manual staining regimens are time-consuming and require careful handling in well-established skin biopsy laboratories to prevent damage or the introduction of artefacts during reagent pipetting and section transfer. Thus, for intra-epidermal nerve fibre quantification to be incorporated into the workflow of a busy diagnostic laboratory, procedures must be reliable and both time and labour efficient with protocols matching the high-volume throughput of diagnostic histopathology services.

Here, we aimed to develop an automated version to improve both accessibility and scalability. The use of automated tinctorial and immunohistochemical staining is becoming increasingly necessary to fulfil the growing number of clinicians' requests.[16,17] Indeed, it has been proposed that immunofluorescent signal intensity could be used as a marker for IENFD.[18] However, immunofluorescence staining signal can fade[19] and there are barriers to implementation of digital pathology.[20] As such, we chose 3,3'-Diaminobenzidine (DAB) as the visualisation method for the present study to match current diagnostic histopathology workflows.

In this study, we detail a quality-assured process for the automated staining of PGP9.5 positive IENFs in skin biopsy sections, which can be optimised for use on other automated immunohistochemistry platforms. We report intra-epidermal nerve fibre densities and the associated inter- and intra-class coefficients of examiners performing intra-epidermal nerve fibre quantification in healthy control participants, people with fibromyalgia syndrome and idiopathic small fibre neuropathy.

2 | MATERIALS AND METHODS

Participants with fibromyalgia syndrome, idiopathic small fibre neuropathy and healthy volunteers were recruited. A priori ethical approval was obtained (North West—Preston Research Ethics Committee—REC reference: 19/NW/0078; South West—Frenchay Research Ethics Committee REC reference: 20/SW/0138) and all participants provided written informed consent. An overview of the automated immunohistochemistry workflow is shown in Figure 1.

3 | PUNCH BIOPSY COLLECTION AND PROCESSING

Participants with fibromyalgia syndrome and healthy volunteers underwent punch biopsies of the proximal thigh, distal lateral thigh and distal leg (Figure 2). Participants with idiopathic small fibre neuropathy underwent punch biopsy at the distal lateral thigh and distal leg only. The distal site was selected in keeping with where published normative reference ranges have been reported.[5] Punch biopsies were performed after local 2% lidocaine injection using sterile technique with a 3 mm disposable circular punch (INSTRAPAC biops, Catalogue number 8181). No sutures were required. Immediately after skin biopsy, specimens were fixed in cold 2% paraformaldehyde-lysine periodate (2% PLP) (Paraformaldehyde: Merck Life Science UK Limited, Dorset, UK, Catalogue number #P6148; Sodium (meta) periodate: Merck Life Science UK Limited, Dorset, UK, Catalogue number 769517; L-Lysine monohydrochloride: Merck Life Science UK Limited, Dorset, UK, Catalogue number 657-27-2) for 24 h at 4°C and then cryoprotected using gradient 10%, 20% and 30% sucrose in phosphate buffered saline (Merck Life Science UK Limited, Dorset, UK, Catalogue number 57-50-1) for 48 h at 4°C.

3.1 | Embedding and cryotomy

Specimens were bisected and embedded transversely in optimum cutting temperature compound (Leica Biosystems, Milton Keynes, UK, Tissue Freezing Media, Catalogue number: #14020108926) filled moulds and snap frozen in liquid nitrogen for serial skip-sectioning on a cryostat (Leica Biosystems, IL, USA, Leica CM1950). Twelve sections at 50 μm were adhered to positively charged adhesive glass slides (ThermoFisher, Loughborough, Leicestershire, UK, Catalogue number: #10149870) from each biopsy site resulting in six sections per slide for analysis and a spare. This allowed for a 50 μm trim between serial sections whilst allowing restaining if there are artefacts in the initial immunohistochemistry staining run.

3.2 | Demonstration of intra-epidermal nerve fibres

Slides were stained on a barcode programmable automated immunohistochemistry platform (Leica Biosystems, IL, USA, Bond RXm Autostainer) using rabbit anti-human PGP9.5 (ThermoFisher, Rockford, IL, USA, Catalogue number #PA5-29012) at 650 ng/mL. Antibody binding sites were visualised using DAB to form insoluble brown polymeric horseradish peroxidase-linker antibody conjugates (Leica Biosystems, IL, USA, Bond Polymer Refine Detection kit DS9800). The staining protocol programme is summarised in Table 1. Each run was validated

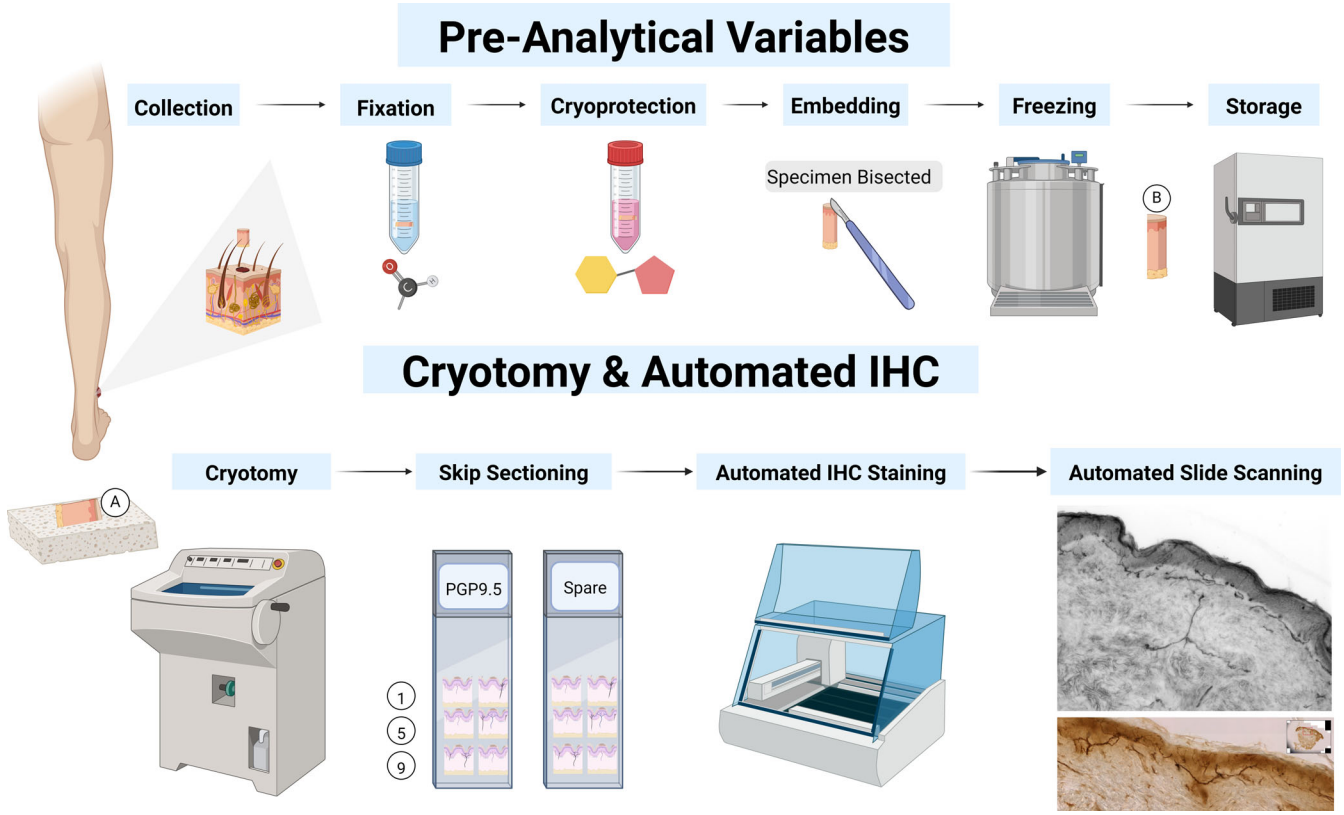

FIGURE 1 The standardised workflow of automated intra-epidermal nerve fibre quantification. Skin biopsies were collected and fixed for 24 h in 2% paraformaldehyde-lysine-periodate and cryo-protected in gradated 10%, 20% and 30% sucrose solution for 48 h. Samples were bisected and embedded transversely in moulds filled with optimum cutting temperature compound and snap frozen in liquid nitrogen. Specimens were kept in labelled cryo-vials with labelled slides stored in slide freezer boxes housed in temperature-monitored −80°C freezers. Skin biopsy sections were trimmed and skip-sectioned on the cryostat with sections picked up on positively charged adhesive glass slides.

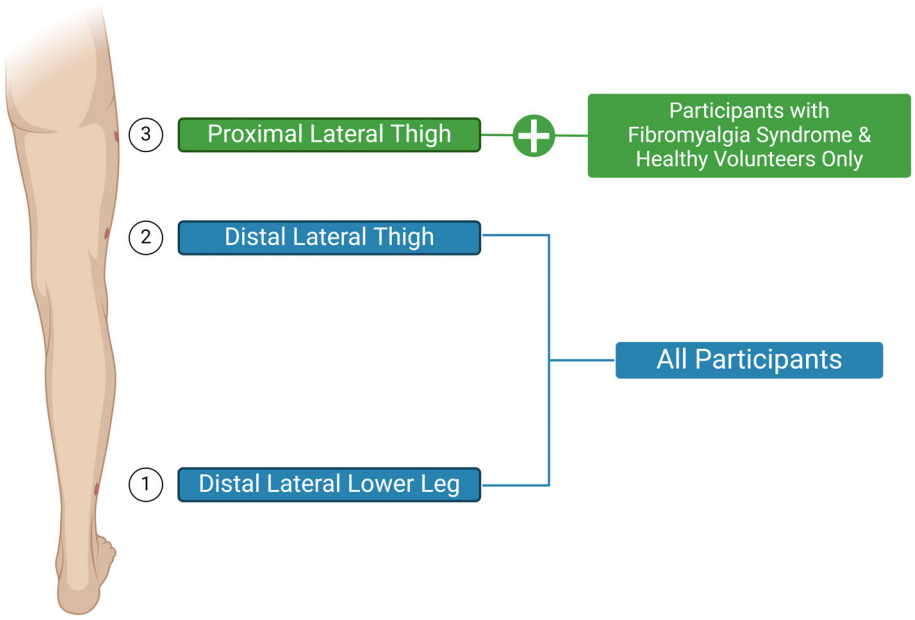

FIGURE 2 The punch biopsy site selection for each study. Participants with idiopathic small fibre polyneuropathy underwent skin biopsy at the distal lateral lower leg 10 cm above the lateral malleolus (1), and the distal lateral thigh 10 cm superior to the upper margin of the patella (2). Participants with fibromyalgia syndrome and healthy volunteers underwent skin biopsy at the distal lateral lower leg 10 cm above the lateral malleolus (1), distal lateral thigh 10 cm superior to the upper margin of the patella (2) and proximal lateral thigh 10 cm below the greater trochanter of the femur.

by a known PGP9.5 positive tissue section and a slide which received all reagents except the primary antibodies acting as a negative control. Slides were coverslipped using an automated coverslipper (Leica Biosystems, IL, USA, CV5030). The sections were imaged using a fully motorised confocal microscope (Carl Zeiss Ltd., Cambridge, UK, Zeiss LSM 800) using Z-stacking and processed into a single image using extended depth of field. Sections for dermis measurement were imaged using an automated slide scanner (Carl Zeiss Limited,

TABLE 1 Automated immunohistochemistry protocol for the demonstration of protein gene product 9.5^{+ve} intra-epidermal nerve fibres.

Reagent	Time (Minutes)	Notes
1% Triton X in TBS	15 (3 × 5)	Permeabilisation
Peroxide Block	15 (1 × 15)	
PGP9.5 (PA529012 [1:400])	360 (3 × 120)	Primary antibody; 100 µL dispensed.
Secondary Detection Polymer	120 (2 × 60)	Secondary antibody and detection
Detection Kit (DAB/Neutral Red)	15 (1 × 5, 1 × 10)	Visualisation
Counterstain	NA	Haematoxylin optional
Option for Multiplex Staining	-	

Abbreviations: DAB, 3,3′-Diaminobenzidine; PGP9.5, protein gene product 9.5; TBS, Tris-buffered saline.

Cambridge, UK, Zeiss Axioscan Z1) (ocular micro-meter calibrated) using a 20x objective (Carl Zeiss Ltd., Cambridge, UK, Zeiss, Plan-Apochromat 20x/NA 0.8). All slides were barcode labelled with their respective study identifier, biopsy site and immunohistochemistry run details and catalogued in number order in slide archive boxes.

3.3 | Quality assurance

Positive and negative control material were assessed to validate a slide run. Slides were assessed to ensure correct tissue orientation and the absence of folds, creases, chatters and scores. Sections which passed quality assurance and control procedures were numbered sequentially from the first to the last viable section and circled to ensure examiner's counts belonged to the same section and to facilitate scanning at different focal depths.

3.4 | Dermis measurement

Processing of whole-section z-stacked images included minimum intensity z-projection and median filtering to obtain cropped black and white images using FIJI,[21] a freely available open source software (https://fiji.sc/). This step was necessary to reduce file size and only preserve the section image after slide scanning. After image processing, specimens were manually measured using FIJI to determine the epidermis length.

3.5 | Intra-epidermal nerve fibre quantification

IENFs were observed by using bright-field microscopy and manually counted at 40x magnification (Olympus, Southend-on-Sea, UK, UPlanFL 40x/ NA 0.75) by two independent examiners in a masked and randomised fashion. Each section was counted by at least two examiners who were researchers associated with this study (JB and LR). Disagreements greater than 10% were arbitrated by an additional examiner (UA). JB received intensive training in intra-epidermal nerve fibre quantification by UA prior to study initialisation. IENFs which cross the papillary dermis-epidermal junction were counted as per the European Federation of Neurological Societies guidelines.[11,22] The IENFD was calculated in at least three sections per site using the total number of IENFs per site divided by the total length of the epidermis (fibres/mm).

3.6 | Statistical analysis

All statistical analyses were performed using R software (version 4.0.2). Differences in intra-epidermal nerve fibre densities between free-floating and automated methods were assessed using the Wilcoxon signed-rank test for matched pairs data. The median difference of IENFD was calculated and non-inferiority of the automated method was determined by the lower confidence limit of the 95% confidence interval for the median difference exceeded a non-inferiority margin of −0.4 fibres/mm. The non-inferiority margin for comparing free-floating and automated methods was based on the smallest difference in the 95th percentile cut-offs for healthy individuals, adjusted for age and sex.[5] To assess the reliability of measurements between and within examiners, intra-class and inter-class correlation coefficients (ICCs) were calculated using the 'irr' package in R.[23] These coefficients and their respective 95% confidence intervals were derived using a mean-rating ($k = 2$) two-way mixed-effects model. ICC values were interpreted according to the guidelines proposed by Koo and Li: ≤0.5 indicates poor reliability, 0.5–0.75 indicates moderate reliability, 0.75–0.9 indicates good reliability and ≥0.9 signifies excellent reliability.[24] In the present study, 'class' refers to the group of observations being measured for consistency, such as IENFD calculations. In addition to the ICC analysis, the mean difference in scores between examiners, standard deviations and intra-epidermal nerve fibre densities were calculated. Differences in IENFD between methods and examiners were evaluated using delta values, representing the differences between paired measurements. Bland–Altman plots were used to visualise delta values against the mean of the paired measurements, providing a graphical representation of the agreement between the methods and examiners providing a visual representation of measurement concordance.

4 | RESULTS

Representative images of the positive control (Figure 3A) and the negative control (Figure 3B), (the latter omitting the primary antibody), clearly delineate the IENFs stained with PGP9.5. An example of a section stained using the automated method which would be counted by the study examiners is shown in Figure 3C to illustrate this process.

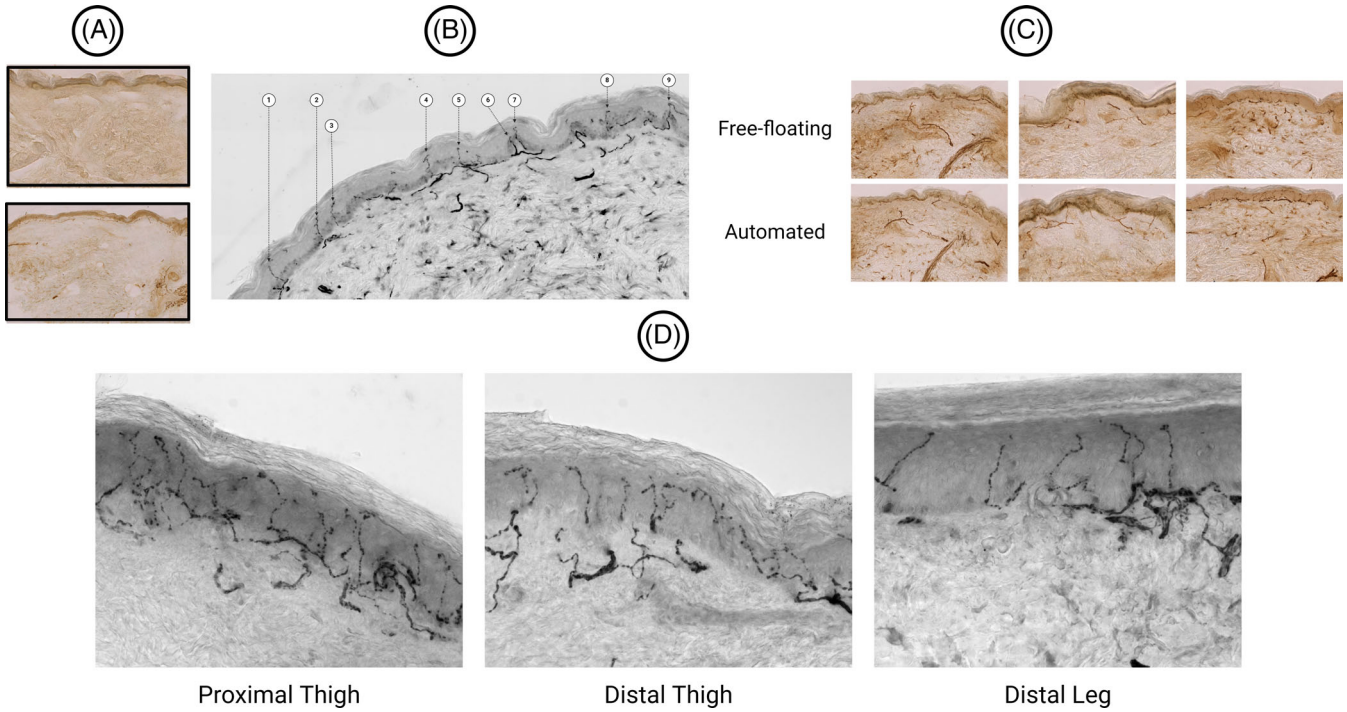

FIGURE 3 Representative scanned images of staining outcomes of sections stained using the free-floating and automated staining methods. (A) Top—representative image of PGP9.5, a negative control section (no primary antibody control); bottom—representative image of a known positive PGP9.5 control section. (B) Photomicrograph prepared using a confocal microscope capturing z-stacked images processed using extended depth of field and median filtering to illustrate the intra-epidermal nerve fibres (IENFs) which would be counted. The IENFD can be calculated per biopsy by counting the total number of IENFs in at least three sections divided by the total length of the epidermis (fibres/mm). (C) Representative images of the staining outcomes between free-floating and automated staining methodologies illustrating their similarity in both quality and intensity. (D) Representative images at 40x magnification using the automated methodology of all sampled anatomical sites of a single participant.

As shown in Figure 3D, the free-floating and automated staining methodologies both yield high-quality staining outcomes in visualising cutaneous nerve fibres.

4.1 | Non-inferiority of free-floating and automated intra-epidermal nerve fibre densities

From nine biopsies, a total of 54 sequential tissue sections were analysed by the same examiner; 27 sections were stained using the free-floating method and 27 via the automated method. As shown in Figure 4 (left), measurements of IENFD from both methods are aligned along the line of equality ($R^2 = .98$). Further, the Bland–Altman plot demonstrates that intra-epidermal nerve fibre densities resided within the predefined limits of agreement (Figure 4; right). The automated method was found to be non-inferior to the manual free-floating method in paired comparison of calculated intraepidermal nerve fibre densities (median difference 0.3; lower 95% confidence interval (CI) −0.00006; $p = .08$). Indeed, the intra-class correlation coefficient 99% (CI: 0.9-1), indicated a high agreement between the free-floating and automated methods. Similarly, the mean (± standard deviation) IENFD were in close agreement (Free-floating: 5.6 ± 3.4 fibres/mm; Automated: 5.9 ± 3.2 fibres/mm).

4.2 | Reliability of intra-epidermal nerve fibre density measurements

IENFD measurements from two examiners and repeat assessments by the same examiner clustered around the line of equality (both $R^2 = .99$; Figure 5A). Bland–Altman plots show measurements fall within the established limits of agreement (Figure 5B). The inter-class correlation coefficients indicate excellent reliability between examiners at 99.7% (CI: 0.99-1) for intra-epidermal nerve fibre densities. The average discrepancy between examiners was minimal, at 0.02 ± 0.4 fibres/mm. Similarly, intra-observer reliability was excellent, shown by an intra-class correlation of 99% (CI: 0.99-1) and a mean difference of 0.06 ± 0.56 fibres/mm in repeated measurements by the same observer.

4.3 | Participant characteristics

The clinical and demographic measures of the 100 participants (FMS, $n = 62$; ISFN, $n = 16$ and HV, $n = 22$) who underwent skin biopsy are shown in Table 2. The idiopathic small fibre neuropathy group were older than the FMS and healthy control groups. There was a greater proportion of females in all groups, which was greatest in the FMS

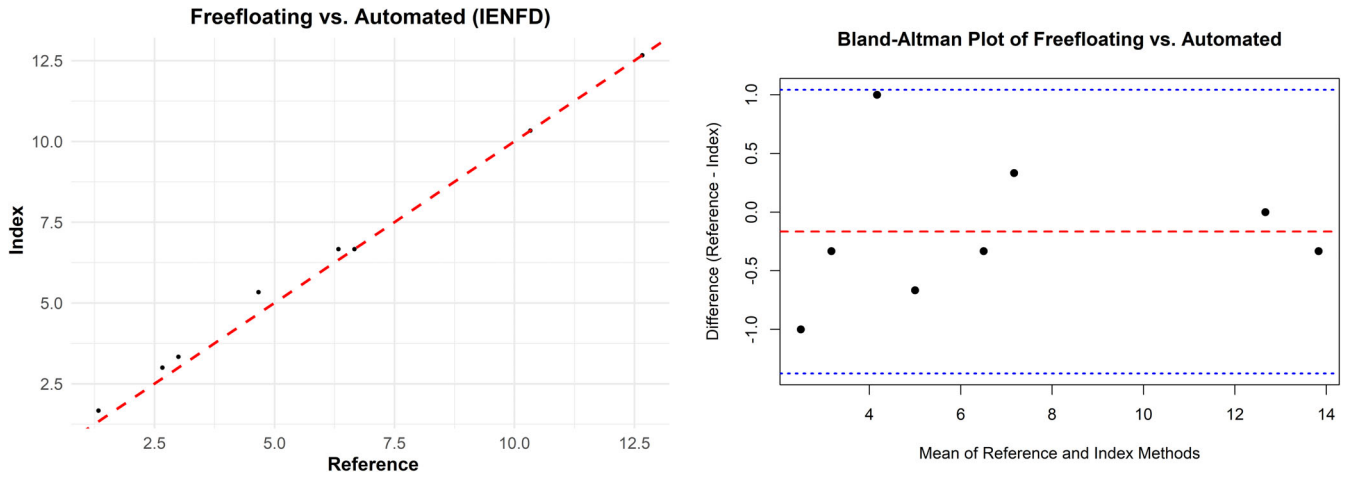

FIGURE 4 Scatter plot and Bland–Altman analysis of intra-epidermal nerve fibre density comparisons between free-floating and automated PGP9.5 staining methods. Left: A scatter plot illustrating the correlation between intra-epidermal nerve fibre densities as quantified by free-floating and automated PGP9.5 staining methods which are aligned along the line of equality ($R^2 = .98$). Right: A Bland–Altman plot to show the delta values are within limits of agreement indicative of similar reported densities between both staining methods. The red dashed line represents the mean difference between the two methods, while the blue dashed lines indicate the limits of agreement, within which 95% of the differences are expected to fall.

group. The fibromyalgia syndrome and idiopathic small fibre neuropathy groups had similar durations of disease and higher blood pressure and body mass index compared to the healthy control group, which were highest in the ISFN group.

4.4 | Skin biopsy findings

A total of 274 punch biopsies were collected and a total of 784 sections were counted. The mean ± standard deviation IENFD of healthy volunteer participants were 11.5 ± 4.0 fibres/mm, 11.9 ± 4.7 fibres/mm and 9.9 ± 4.6 fibres/mm at the proximal thigh, distal lateral thigh and distal leg, respectively. The IENFD of participants with fibromyalgia syndrome was 8.5 ± 4.4, fibres/mm, 7.9 ± 4.6, fibres/mm and 7.2 ± 3.7 fibres/mm at the proximal thigh, distal lateral thigh and distal leg, respectively. The IENFD of participants with idiopathic small fibre neuropathy was 6.5 ± 3.5 fibres/mm and 2.6 ± 2.2 fibres/mm at the distal lateral thigh and distal leg, respectively. While it was anticipated that more proximal sites have a higher IENFD, our findings indicate slightly higher values at the distal thigh relative to the proximal thigh, which could be attributed to individual variability or sampling differences. Automated immunohistochemistry-stained tissue sections of IENFs in healthy volunteers, participants with fibromyalgia syndrome and those with idiopathic small fibre neuropathy are shown in Figure 5C.

5 | DISCUSSION

We have successfully adapted an established research and clinical technique into a method which may be implemented into the workflow of a routine histopathology laboratory. To our knowledge, this is the first demonstration of the automation of intra-epidermal nerve fibre assessment using thick 50 µm sections and polymer DAB visualisation methodology. We demonstrate excellent inter- and intra-observer agreement in intra-epidermal nerve fibre quantification from automated slide preparations. Skin biopsy processing and intra-epidermal nerve fibre assessment are labour intensive and automated, high-volume throughput is necessary for use in a dedicated neuropathology reference laboratory. The present study demonstrates a workflow which can also be implemented in a specialised neuropathology laboratory and may also be transferred to immunofluorescence techniques. The IENFD data generated are consistent with the published literature of studies using manual techniques, with the healthy volunteer participant values falling within the normative reference values at the distal leg[5] with lower values in fibromyalgia syndrome and idiopathic small fibre neuropathy. The reliability and reproducibility of intra-epidermal nerve fibre quantification in the present study is similar to earlier published data using manual free-floating staining methodology.[4,25,26]

Dermis measurement at scale requires a pixel classifier or tissue recognition software to measure the dermis in a semi-automated manner in scanned slides. Semi-automated nerve counting is possible in DAB and fluorescence visualised sections.[27] Key limitations for automated nerve fibre quantification are section thickness, processing, freezing and cutting artefact and variability in manual staining outcomes. Standardisation of high quality cryosections for automated visualisation of IENFs could mitigate variability and increase reproducibility.

Whilst this study is proof-of-concept, validation of these findings in a reference laboratory may prove useful for accreditation and use in clinical research. Indeed, the Royal College of Pathologists have

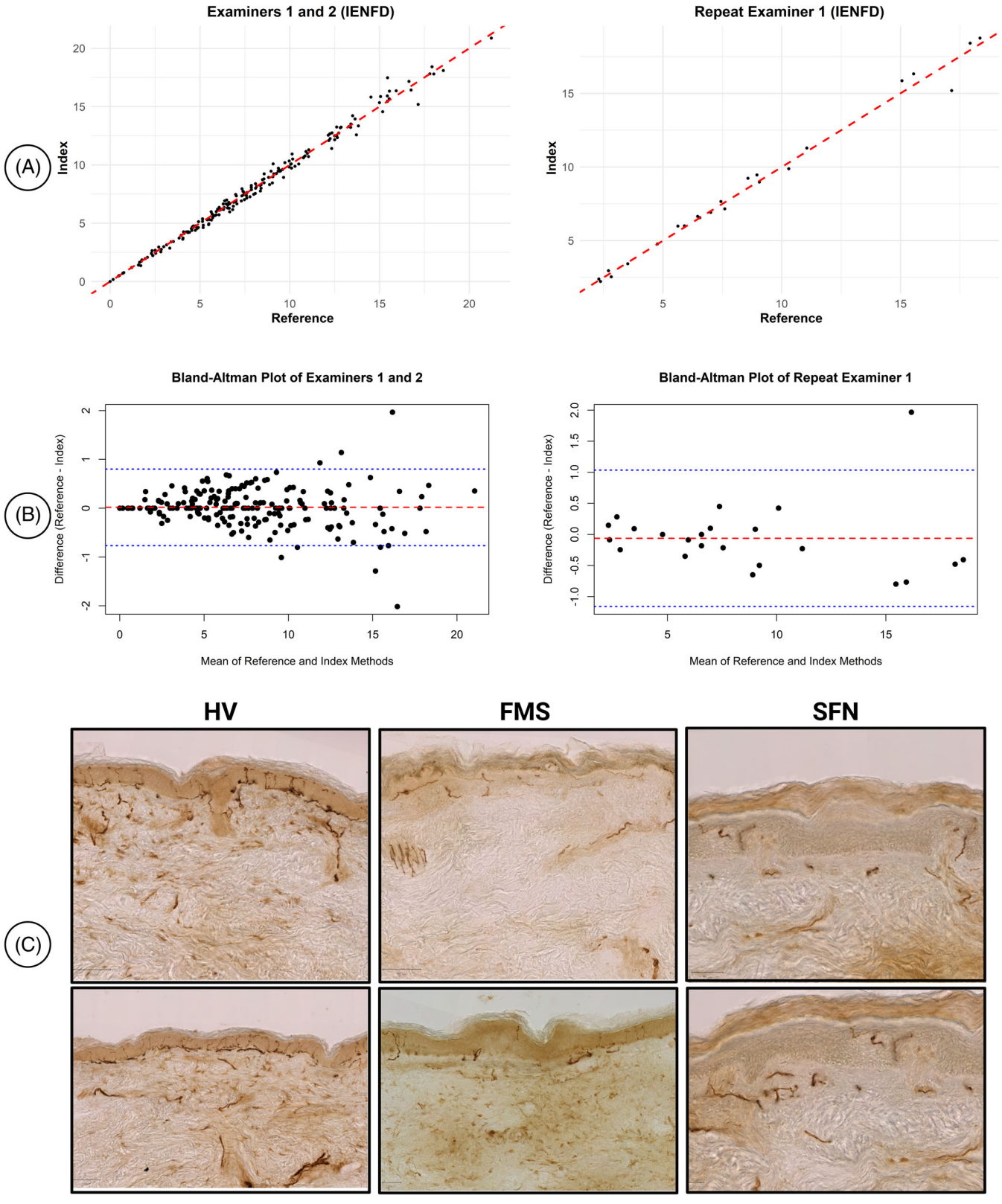

FIGURE 5 Legend on next page.

recently included IENFD assessment as part of the neuropathology tissue pathway.[28]

As a proof-of-concept study, we did not formally collect data on laboratory personnel engagement, total procedure time, quality assurance pass rates and restained section numbers. These aspects, in addition to cost analysis, scalability and the impact of this method on costs and turnaround time, will be addressed in future studies. To transition this proof-of-concept study to a properly powered comparison study, a sample size of 175 would be required to compare manual and automated IENFD methodologies. We would expect that this study should incorporate a detailed cost analysis to include initial investment, operational costs, and time-efficiency of laboratory staff for both methods. Furthermore, economic modelling throughout the duration of the study would allow for comparison between cost-benefit and return on investment. We would anticipate that these data would allow an evaluation of whether the automated method has a significant impact on both accessibility and reliability. Establishing these parameters is essential for the adoption of automated IENFD as a clinical standard which could substantiate this technique for the diagnosis of small fibre neuropathies. Moreover, a limitation of the current study is the lack of a blinded parallel proficiency test comparing manual free-floating and automated methods across different disease groups with an independent diagnostic IENFD laboratory. Furthermore, a comprehensive analysis is warranted considering differences in tissue characteristics and variability of biological tissues. Moreover, the heterogeneous composition of IENFs due to inter-individual morphological and pathological gradients of nerve loss in patients with small fibre neuropathy should be considered to ensure that automated methods are effective at detecting severe denervation.[29] The implementation of this method requires on-board positive and negative controls on each slide, which may pose challenges for diagnostic laboratories.[30] Difficulties may also arise from the need for control tissue to undergo the same pre-analytical conditions such as choice of fixative and duration of processing. A systematic approach is needed for selecting PGP9.5 positive tissues to undergo the same preparation as skin samples for the detection of PGP9.5 positive IENFs until an efficient workflow for wax-based preparations can be found. Despite these challenges, a diagnostic lab could mitigate these issues by systematically collecting skin biopsies identified as benign skin lesions, and epithelial cells in mastectomy and nephrectomy specimens, which will likely provide a dependable source of control material.

TABLE 2 Clinical and demographic measures in participants.

Variable	HV, $n = 22^1$	FMS, $n = 62^1$	ISFN, $n = 16^1$
Age (Years)	43.3 (14.3)	46.4 (15.3)	57.8 (10.9)
Female—n, %	20, 64.5%	54, 88.5%	9, 56.3%
Years Since Diagnosis	0 (0)	7.3 (6.7)	6.7 (5.4)
Systolic BP (mmHg)	126.6 (16.1)	132.6 (19.1)	132.9 (24.3)
Diastolic BP (mmHg)	78.9 (11.7)	82.1 (13.1)	84.7 (15.9)
BMI	28.2 (5.7)	29.6 (7)	31.1 (6.7)
HbA1c mmol/mol	37.0 (4.2)	35.8 (4.7)	38.0 (2.9)
Cholesterol mmol/l	5.0 (1.2)	5.1 (1)	4.2 (1.9)
Triglycerides mmol/l	1.2 (0.5)	1.7 (0.9)	1.1 (0.6)
IENFD Proximal Thigh	11.5 (4.5)	8.5 (4.4)	NA
IENFD Distal Thigh	11.9 (4.7)	7.9 (4.6)	6.5 (3.5)
IENFD Distal Leg	9.9 (4.6)	7.2 (3.7)	2.6 (2.2)
Number of biopsies—n	66	178[a]	32

Note: 1 = Mean ± Standard Deviation (SD) unless otherwise indicated.
Abbreviations: BMI, body mass index; FMS, fibromyalgia syndrome; HV, healthy volunteer; ISFN, idiopathic small fibre neuropathy; mmHg, millimetres of mercury; mmol, millimole; mol, mole.
[a]Four participants with fibromyalgia syndrome experienced syncope, preventing completion of biopsy collection at all sites.

FIGURE 5 Scatter plot, Bland–Altman analysis across examiners and representative staining outcomes of included participants. (A) Scatter plots illustrating the correlation between intra-epidermal nerve fibre densities as quantified by examiners 1 and 2 (left) and repeated quantification by examiner 1 (right) are both clustered around the line of equality (both $R^2 = .99$). (B) Bland–Altman plots of inter- (left) and intra-observer (right) delta values of IENFD. The majority of data points fall within the limits of agreement, indicating a high level of concordance between examiner 1 and 2 and repeat counts by examiner 1. The red dashed line represents the mean difference between the two methods. The blue dashed lines indicate limits of agreement, within which 95% of the differences are expected to fall. (C) Representative staining outcomes of healthy volunteers (HV; left), participants with fibromyalgia syndrome (FMS; middle) and small fibre neuropathy (SFN; right) of sections stained using the automated staining method.

6 | CONCLUSION

This study demonstrates that a standardised, automated protocol for detecting cutaneous nerve fibres in skin biopsies is non-inferior to the established manual technique. Biopsies from 100 participants yielded consistent and reliable IENFD measurements. Given these results, the automated method offers a promising avenue to facilitate broader adoption in clinical and research settings for the assessment of peripheral neuropathies.

AUTHOR CONTRIBUTIONS

All named authors meet the International Committee of Medical Journal Editors (ICMJE) criteria for authorship for this article, take responsibility for the integrity of the work and have given their approval for this version to be published. All persons who meet authorship criteria are listed as authors.

ACKNOWLEDGEMENTS

We thank the Liverpool Ocular Oncology Research Group (LOORG) for technical assistance when using the Leica Bond RXm for immunohistochemical analyses. We also appreciate the Liverpool Centre for Cell Imaging (CCI) and the Histology Shared Research Facilities for their technical support. We also acknowledge the contribution of laboratory technical assistance of Samuel Thomas. All figures created by Jamie Burgess using BioRender.com.

FUNDING INFORMATION

J.B. received a PhD studentship from the Pain Relief Foundation. Participants with fibromyalgia syndrome and healthy volunteers were included from DEFINE-FMS funded by Versus Arthritis (Grant number 22471). Participants with idiopathic small fibre neuropathy were included as part of the 'Defining small fibre neuropathy and neuropathic pain in idiopathic fibre neuropathy and chemotherapy-induced peripheral neuropathy' study.

DATA AVAILABILITY STATEMENT

The data that support the findings of this study are available from the corresponding author upon reasonable request.

ORCID

Jamie Burgess https://orcid.org/0000-0002-7165-6918
Rayaz A. Malik https://orcid.org/0000-0002-7188-8903

REFERENCES

1. Thomas S, Enders J, Kaiser A, et al. Abnormal intraepidermal nerve fiber density in disease: a scoping review. *Front Neurol*. 2023;14:1161077.
2. Raicher I, Ravagnani LHC, Correa SG, Dobo C, Mangueira CLP, Macarenco R. Investigation of nerve fibers in the skin by biopsy: technical aspects, indications, and contribution to diagnosis of small-fiber neuropathy. *Einstein (Sao Paulo)*. 2022;20:eMD8044.
3. Sina B, Kao GF, Deng AC, Gaspari AA. Skin biopsy for inflammatory and common neoplastic skin diseases: optimum time, best location and preferred techniques. A critical review. *J Cutan Pathol*. 2009;36:505-510.
4. McArthur JC, Stocks EA, Hauer P, Cornblath DR, Griffin JW. Epidermal nerve fiber density: normative reference range and diagnostic efficiency. *Arch Neurol*. 1998;55:1513-1520.
5. Lauria G, Bakkers M, Schmitz C, et al. Intraepidermal nerve fiber density at the distal leg: a worldwide normative reference study. *J Peripher Nerv Syst*. 2010b;15:202-207.
6. Devigili G, Rinaldo S, Lombardi R, et al. Diagnostic criteria for small fibre neuropathy in clinical practice and research. *Brain*. 2019;142:3728-3736.
7. Freeman R, Gewandter JS, Faber CG, et al. Idiopathic distal sensory polyneuropathy: ACTTION diagnostic criteria. *Neurology*. 2020;95:1005-1014.
8. Lauria G, Hsieh ST, Johansson O, et al. European Federation of Neurological Societies/peripheral nerve society guideline on the use of skin biopsy in the diagnosis of small fiber neuropathy. Report of a joint task force of the European Fe-deration of neurological societies and the peripheral nerve society. *Eur J Neurol*. 2010d;17:903-e949.
9. Lauria G. Recent developments in the management of peripheral neuropathy using skin biopsy. *Revue Neurol*. 2007;163:1266-1270.
10. Lauria G, Cazzato D, Porretta-Serapiglia C, et al. Morphometry of dermal nerve fibers in human skin. *Neurology*. 2011;77:242-249.
11. Lauria G, Cornblath DR, Johansson O, et al. EFNS guidelines on the use of skin biopsy in the diagnosis of peripheral neuropathy. *Eur J Neurol*. 2005a;12:747-758.
12. Lauria G, Dacci P, Lombardi R, et al. Side and time variability of intraepidermal nerve fiber density. *Neurology*. 2015;84:2368-2371.
13. Lauria G, Faber CG, Cornblath DR. Skin biopsy and small fibre neuropathies: facts and thoughts 30 years later. *J Neurol Neurosurg Psychiatry*. 2022;93:915-918.
14. Lauria G, Lombardi R. Skin biopsy: a new tool for diagnosing peripheral neuropathy. *Bmj*. 2007;334:1159-1162.
15. Lauria G, Lombardi R, Borgna M, et al. Intraepidermal nerve fiber density in rat foot pad: neuropathologic-neurophysiologic correlation. *J Peripher Nerv Syst*. 2005c;10:202-208.
16. Grogan T, Reinhardt K, Jaramillo M, Lee D. An update on "special stain" Histochemistry with emphasis on automation. *Adv Anat Pathol*. 2000;7:110-122.
17. Osaro E, Chima N. Challenges of a negative work load and implications on morale, productivity and quality of service delivered in NHS laboratories in England. *Asian Pac J Trop Biomed*. 2014;4:421-429.
18. Corrà MF, Sousa M, Reis I, et al. Advantages of an automated method compared with manual methods for the quantification of Intraepidermal nerve fiber in skin biopsy. *J Neuropathol Exp Neurol*. 2021;80:685-694.
19. Dikicioglu E, Meteoglu I, Okyay P, Culhaci N, Kacar F. The reliability of long-term storage of direct immunofluorescent staining slides at room temperature. *J Cutan Pathol*. 2003;30:430-436.
20. Randell R, Ruddle RA, Treanor D. Barriers and facilitators to the introduction of digital pathology for diagnostic work. *Stud Health Technol Inform*. 2015;216:443-447.
21. Schindelin J, Arganda-Carreras I, Frise E, et al. Fiji: an open-source platform for biological-image analysis. *Nat Methods*. 2012;9:676-682.
22. Lauria G, Hsieh ST, Johansson O, et al. European Federation of Neurological Societies/peripheral nerve society guideline on the use of skin biopsy in the diagnosis of small fiber neuropathy. Report of a joint task force of the European Federation of Neurological Societies and the peripheral nerve society. *Eur J Neurol*. 2010c;17:903-912. e944-909.
23. Gamer M, Lemon J, Fellows I, Singh P. Irr: various coefficients of interrater reliability and agreement. 2019. R package version 0.84.1. Available at: https://cran.r-project.org/web/packages/irr/index.html
24. Koo TK, Li MY. A guideline of selecting and reporting Intraclass correlation coefficients for reliability research. *J Chiropr Med*. 2016;15:155-163.
25. Gøransson LG, Mellgren SI, Lindal S, Omdal R. The effect of age and gender on epidermal nerve fiber density. *Neurology*. 2004;62:774-777.

26. Smith AG, Howard JR, Kroll R, et al. The reliability of skin biopsy with measurement of intraepidermal nerve fiber density. *J Neurol Sci*. 2005;228:65-69.
27. Seger S, Stritt M, Doppler K, et al. A semi-automated method to assess intraepidermal nerve fibre density in human skin biopsies. *Histopathology*. 2016;68:657-665.
28. Brandner SH, Jaunmuktane M, Phadke Z, et al. *G101: Tissue Pathways for Non-Neoplastic Neuropathology Specimens*. The Royal College of Pathologists; 2023.
29. Piscosquito G, Provitera V, Mozzillo S, et al. The analysis of epidermal nerve fibre spatial distribution improves the diagnostic yield of skin biopsy. *Neuropathol Appl Neurobiol*. 2021;47:210-217.
30. Torlakovic EE, Francis G, Garratt J, et al. Standardization of negative controls in diagnostic immunohistochemistry: recommendations from the international ad hoc expert panel. *Appl Immunohistochem Mol Morphol*. 2014;22:241-252.

How to cite this article: Burgess J, Marshall A, Rapteas L, et al. Automated immunohistochemistry of intra-epidermal nerve fibres in skin biopsies: A proof-of-concept study. *J Peripher Nerv Syst*. 2024;29(3):329-338. doi:10.1111/jns.12650